

PACS numbers: 52.50.Jm; 52.38.Ph
DOI: 10.1070/QE2013v043n09ABEH015168

Temporal structure of X-ray radiation pulses of picosecond laser plasma

V.S. Belyaev, D.V. Kovkov, A.P. Matafonov, G.F. Karabadzhak, G.G. Raikunov, A.Ya. Faenov, S.A. Pikuz, I.Yu. Skobelev, T.A. Pikuz, D.A. Fokin, G.N. Ignat'ev, S.V. Kapitanov, P.S. Krapiva, K.E. Korotkov, V.E. Fortov

Abstract. **The shape of the X-ray pulse generated by picosecond laser plasma is experimentally studied. The unusual phenomenon was experimentally observed for the first time for targets made of moderate-heavy chemical elements, namely, the pulse of hard X-ray radiation generated by laser plasma at the laser radiation flux of $\sim 10^{18}$ W cm^{-2} had a longer duration than the pulse of softer X-ray radiation. A simple kinetic model is suggested for explaining this fact. We have suggested a method for controlling the temporal shape of X-ray pulse emitted by laser plasma by varying the contrast of laser pulse.**

Keywords: *laser plasma, X-ray radiation, picosecond pulses.*

1. Introduction

Laser plasma is a powerful source of short-wavelength radiation and can be successfully employed in various applications (see, for example, [1–22]). Numerous works have been devoted to studying the spectral and energy characteristics of X-ray plasma radiation. Up to now, sufficiently detailed information has been obtained concerning time-integrated radiation characteristics of laser plasma. On the contrary, no thorough investigations of the temporal characteristics of short-wavelength radiation of laser plasma have been performed yet. This refers to the case of laser plasma produced by high-power pico- and sub-picosecond laser pulses. Just a few works can be mentioned (see, for example, [23–30]), in which the emission spectra were recorded in narrow soft X-ray spectral ranges with the pico- and sub-picosecond resolution. In those cases, comparatively light chemical elements were used in targets (mainly Mg, Al, Si), which, obviously, is not optimal from the viewpoint of producing a bright source of X-ray radiation. Seemingly, only in [30] the dependence of duration of laser plasma glow in the soft X-ray range ($\lambda \sim$ 50 Å) on the laser pulse intensity and contrast was investigated for both light (Al) and heavy (Au) targets.

The results of these works show that the duration of the X-ray pulse emitted by laser plasma in different experiments may vary from a fraction of unity or unity [23, 25] to dozens [28, 29] and even hundred [23, 24, 27] picoseconds; however, the question what factors determine this duration has not actually been raised.

Nevertheless, it is important to know the temporal shape of X-ray pulse generated by laser plasma in a number of possible applications. For example, in radiography of fast processes (shock waves in condensed media and so on) the duration of the X-ray pulse determines the temporal resolution of radiography method. It is also important to know the shape of the X-ray pulse for solving problems of laboratory astrophysics in modelling by laser plasma astrophysical sources of short-wavelength radiation and the results of its action on a substance in various aggregate states including the plasma state.

In addition to information on the temporal shape of generated pulse, control of this shape is needed in many applications. From general considerations it is clear that various approaches, more or less obvious, can be used for this purpose. For example, it is obvious that by reducing the size of the focused laser radiation spot on a target the duration of the X-ray pulse emitted by laser plasma can be shortened due to faster cooling. It is natural that a variation in the laser pulse duration in certain limits will affect the duration of the X-ray pulse radiation emitted by plasma. There are also less obvious factors affecting the time shape of the pulse generated by laser plasma (one of such factors is considered in the present work). However, the possibility to control the temporal shape of a short-wavelength pulse generated by laser plasma actually has not been studied yet.

In the present work, the temporal shape of a short-wavelength pulse emitted by picosecond laser plasma was experimentally investigated. For the first time, a possible method is considered for controlling the pulse temporal shape by varying the laser pre-pulse amplitude or the laser pulse contrast.

2. Scheme of the experiment and diagnostic methods

Experiments were performed by using the 10-TW 'Neodim' laser installation (TsNIIMash, Korolyov). The scheme of the experiments is shown in Fig. 1. The laser pulse at the wavelength of 1.055 μm had the energy of 10 J at the duration of 1.5 ps.

The laser beam was focused by the off-axes parabolic mirror with the focal distance of 20 cm onto the surface of a

V.S. Belyaev, D.V. Kovkov, A.P. Matafonov, G.F. Karabadzhak, G.G. Raikunov Federal State Unitary Enterprise 'Central Research Institute of Machine Building' (TsNIIMash), ul. Pionerskaya 4, 141070 Korolyov, Moscow region, Russia; e-mail: vadimbelyaev@mtu-net.ru;
A.Ya. Faenov, S.A. Pikuz, I.Yu. Skobelev, T.A. Pikuz, D.A. Fokin, V.E. Fortov Joint Institute for High Temperatures, Russian Academy of Sciences, ul. Izhorskaya 13, Bld. 2, 125412 Moscow, Russia; e-mail: faenov@ihed.ras.ru, igor.skobelev@gmail.com, fortov@ficp.ac.ru;
G.N. Ignat'ev, S.V. Kapitanov, P.S. Krapiva, K.E. Korotkov All-Russian Institute of Automatics, ul. Luganskaya 9, 115304 Moscow, Russia

Received 4 March 2013; revision received 28 May 2013
Kvantovaya Elektronika **43** (9) 865–870 (2013)
Translated by N.A. Raspopov

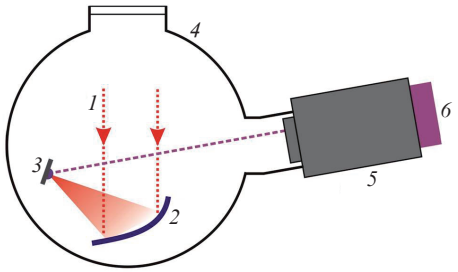

Figure 1. Scheme of the experiment: (*1*) radiation of picosecond laser; (*2*) off-axis parabolic mirror; (*3*) solid target; (*4*) vacuum chamber with flanges; (*5*) detector CXP8; (*6*) CCD-camera with a SFER11.02.000 sensor.

solid-state target at an angle of 40° to its normal. The focusing system provided a peak intensity of $\sim 2 \times 10^{18}$ W cm^{-2} (the laser spot diameter was ~15 μm). The shape of soft X-ray radiation (SXR) generated by plasma ($E_{phot} < 10$ keV) was measured by an X-ray chronograph recorder CXP8 (All-Russia Institute of Automatics, Moscow) that was installed symmetrically to the target normal at the same angle to it. For the target we employed a 2-mm-thick plane copper plate. The expected time resolution of the CXP8 recorder was 2 ps. The spectral range of the recorder was determined by filters made of polypropylene films (with the total thickness of 2 μm) and by the efficiency of the gold cathode (a layer of Au with a thickness of 300 Å deposited to a 1-mm-thick polypropylene film). In most experiments this range was 0.1–10 keV (spectral transmission data were taken from the Internet at http://henke.lbl.gov/optical_constants/). The additional 10-μm-thick Al filter reduced the detection range to 1–10 keV.

An optical image from the screen was recorded by the CCD-camera with a SFER11.02.000 sensor (developed by the All-Russia Institute of Automatics), which was started by a generator triggered by elements of the laser complex.

Figure 2 shows the chronograms of laser plasma SXR pulses, obtained in the spectral ranges 0.1–10 keV and 1–10 keV.

In the present work we investigated the dependence of time characteristics of SXR pulses on the contrast of the laser pulse $K = I_{pulse}/I_{pre}$ which is equal to the ratio of the main laser pulse intensity to the pre-pulse intensity. Since the laser pulse had two pre-pulses – the picosecond one arising 13 ns prior to the main pulse and the pre-pulse of amplified spontaneous emission with the duration of 4 ns directly adjacent to the main pulse – we will speak about two contrasts of the laser pulse denoted by K_{13ns} and K_{ASE}, respectively. For convenience, we will call the second pre-pulse 'pedestal' (the term is often employed) and the first one will be termed simply 'pre-pulse'.

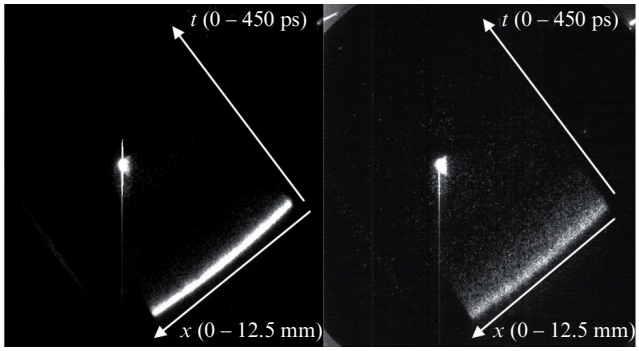

Figure 2. Pulses of soft X-ray radiation at the scale of 0.5 ns in the spectral range 0.1–10 keV (left) and 1–10 keV (right). The slit image evolves diagonally from bottom to top. Bright spots are the result of direct light exposure of the phosphor screen of X-ray image tube by the X-ray radiation pulse.

The durations of SXR pulses determined with CXP8 by the levels 0.1 and 0.5 in various experiments were 31–130 and 16–56 ps, respectively. Examples of recorded profiles of SXR pulses are given in Section 3.

3. Interpretation of experimental data

3.1. Theoretical model

From the data given above one can see that in the X-ray range plasma radiates for at most 100 ps. In this time lapse, at a typical ion expansion velocity of $\sim 10^7$ cm s^{-1} plasma expands by 10 μm, which is less than its initial dimension determined by the focused spot. This means that in developing the theoretical model for a qualitative description of observed behaviour one can neglect the gas-dynamic motion of plasma.

The scenario of plasma heating is presented as follows. First, the pre-plasma is produced under the action of the laser pre-pulse on the target, in which the density profile monotonically decreasing with distance from the target is formed. Since the pre-pulse advance is ~13 ns, in this time lapse plasma noticeably expands and in some regions its electron density reduces to the critical value, that is, to $\sim 10^{21}$ cm^{-3}. The temperature of the pre-plasma may be both low (at a high contrast of the laser pulse) and rather high (at a low contrast). Generally speaking, the pre-plasma temperature should depend on time and follow the pre-pulse time profile. Since the pre-pulse intensity rises slowly we will assume the pre-plasma temperature independent of time and equal to T_0. The consequences of this simplification will be discussed later.

As the main pulse approaches, in the region of critical-density plasma, where the pulse radiation is mainly absorbed, the plasma temperature increases stepwise to the value T_1 greatly exceeding T_0. However, the plasma density in the time scale on the order of dozens picoseconds would not change due to the gas-dynamic motion, as mentioned above. A small variation in the electron density is possible due to the increasing degree of plasma ionisation. With targets comprising multi-electron atoms this effect is negligible, because external electron shells ionised by the pre-pulse have much more electrons than internal shells and an increase in plasma temperature cannot substantially raise the degree of ionisation. Note that with light ions this effect is also significant because pre-plasma in this case is totally ionised and a further increase in the degree of ionisation is not possible.

Thus, we will consider plasma with the following parameters: $T_e = T$ at $t < \tau_{pre}$, $T_e = T_1$, at $t > \tau_{pre}$, $N_e = N_0 = 10^{21}$ cm^{-3} at all values of t.

Undoubtedly, this model is rather simple and pretends only to qualitative explanation of obtained experimental results. Nevertheless, we will see later that it gives a sufficiently adequate quantitative description of the experiment.

Radiation of copper plasma was experimentally detected in two spectral ranges: from 0.1 to 10 keV and from 1 to

10 keV. The experiments showed that the absolute value of soft X-ray radiation pulse is by an order of magnitude greater than that of hard radiation. For copper ions, most bright spectral lines in the range 0.1–10 keV are those related to resonance transitions of type $1s^22l^83l^n4l - 1s^22l^83l^{(n+1)}$ in ions Cu XII–Cu XIX. In the hard range, the most intensive are resonance lines of the transition $1s^22l^73l - 1s^22l^8$ of Ne-like CuXX, which is the L-shell ion. Note that typical spectra of such transitions are given in [31–34] for the cases of copper and zinc targets heated, among other methods, by a picosecond laser pulse. Hence, we will consider the kinetic model with four ions numbered from 0 to 3. We will assume that the radiation in the range 0.1–10 keV is caused by the transitions in the ion with index 1, whereas the harder radiation in the range 1–10 keV is related to the spectral lines of ion with index 2. Hence, the first ion presents some averaged M-ion, and the second ion is first from L-ions, that is, CuXX. In what follows, we will assume that ions with indices 0 and 3 do not contribute into radiation. For the ion with index 3, which actually is the F-like ion CuXXI, such assumption is reasonable because at moderate temperatures it radiates noticeably weaker than the Ne-like ion CuXX. The ion with index 0 will present an average low-charge M-ion which, being ionised, produces M-ions emitting in the considered spectral range.

In the system of kinetic equations for the populations N_i of ground ion states it is necessary to take into account ionisation processes only, because recombination will only be important at the stage of plasma gas-dynamic expansion, that is, at noticeably longer times:

$$\frac{dN_0}{dt} = -N_0 W_{01},$$

$$\frac{dN_1}{dt} = N_0 W_{01} - N_1 W_{12}, \qquad (1)$$

$$\frac{dN_2}{dt} = N_1 W_{12} - N_2 W_{23},$$

where W_{ik} are the probabilities of electron-impact ionisation. According to the Seaton formula (see, for example, [35]) they can be written in the form

$$W_{ik} = 4.3 \times 10^{-8} m N_e (\mathrm{Ry}/E_{ik})^{3/2} \beta^{-1/2} e^{-\beta}, \quad \beta = E_{ik}/T_e, \qquad (2)$$

where E_{ik} is the ionisation potential for ion i; Ry = 13.6 eV; and m is the number of electrons in the valence shell.

By assuming that at the initial instant all ions are in state 0, that is, $N_0(0) = N$ one can write the solution for system (1) as follows:

$$N_1(t) = N\frac{W_{01}}{W_{12} - W_{01}}(e^{-W_{01}t} - e^{-W_{12}t}) + N_1(0)e^{-W_{12}t}, \qquad (3)$$

$$N_2(t) = N\frac{W_{01}W_{12}}{W_{12} - W_{01}}\left(\frac{e^{-W_{01}t} - e^{-W_{23}t}}{W_{23} - W_{01}} - \frac{e^{-W_{12}t} - e^{-W_{23}t}}{W_{23} - W_{12}}\right)$$

$$+ N_2(0)e^{-W_{23}t} + \frac{N_1(0)}{W_{12} - W_{23}}(e^{-W_{23}t} - e^{-W_{12}t}).$$

Plasma radiation is proportional to the populations of ground ion states; hence, in what follows we will assume that the time profile of the SXR pulse coincides with the profiles $N_i(t)$ of pulses emitting in the corresponding spectral range.

Recall that N_1 in (3) presents the ion emitting in the range 0.1–10 keV, whereas N_2 is the ion emitting in the range 1–10 keV. Generally speaking, it is possible to take into account all possible M-ions in (1) but, because their ionisation probabilities are close, this would only 'spread' the concentration of ion N_1 over several states. Since the sum of concentrations of all M-ions is important for the radiation intensity, the final result would be weakly affected, and the analytical solution would not be obvious. Nevertheless, such a more precise consideration of the kinetic model is possible, but it is reasonable only if the time profile of the laser pre-pulse is simultaneously taken into account and a transfer is made from analytical to numerical solution of system (1) with time-dependent factors.

As we will show below, the analytical solution (3) for system (1) allows one to qualitatively (and even quantitatively) interpret the results of performed measurements and to understand which laser pre-pulse characteristics affect the time profile of the SXR pulse generated by laser plasma.

3.2. Duration of plasma glow in different spectral ranges

First consider experiments performed at a maximal possible contrast of the laser pre-pulse (Fig. 3). In this case, a pre-plasma is also produced, but its temperature is rather low so that the pre-plasma definitely does not contribute into the SXR pulse. In the model considered above, this case corresponds to $T_0 \to 0$, $N_0(0) = N$ and $N_1(0) = N_2(0) = 0$.

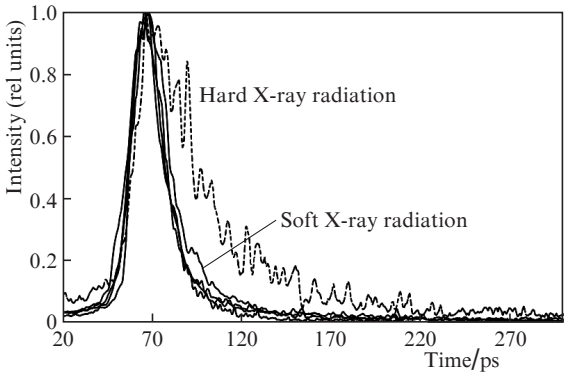

Figure 3. Shape of soft (the range of 0.1–10 keV) and hard (1–10 keV) X-ray pulses emitted by picosecond laser plasma at maximal laser contrasts $K_{13ns} = 2 \times 10^7$ and $K_{ASE} = 10^8$. Soft X-ray radiation pulse was detected in four experiments, the absolute value of the pulse was by above an order of magnitude greater than that of the hard radiation pulse.

First of all one can see from (3) that the growth of ground state population for ion i is related to the rate of ionisation process $(i-1) \to i$, and the subsequent decrease is related with the rate of ionisation $i \to (i+1)$. As long as the ion state corresponds to M-shell these rates gradually fall as i increases. This means that the durations of leading and trailing edges of SXR pulse will be close, but the trailing edge will be somewhat longer.

In transferring from M- to L-shell, a sharp fall in the ionisation rate occurs. This means that the glow of Ne-like CuXX at a fixed temperature should have a slightly longer leading edge ($W_{i-1,i}$ for CuXX is slightly less than for CuXIX) and much

longer trailing edge because $W_{i,i+1}$ for CuXX is much less than for CuXIX. This is well seen in comparing Figs 4 and 5, where the time profiles of concentrations for ions CuXIX and CuXX are presented, which were calculated for various temperatures T_1. The values of ionisation potentials for copper included in (3) were taken from SPECTR-W^3 database [36].

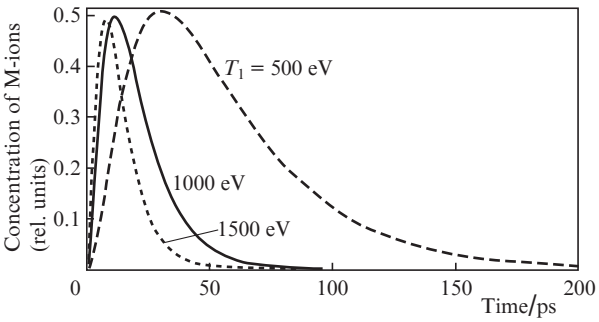

Figure 4. Time profiles of CuXIX ion concentration calculated for various values of T_1.

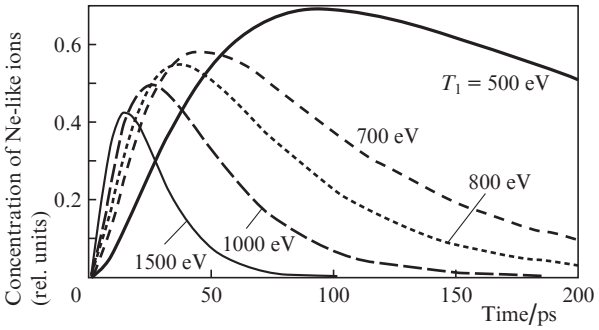

Figure 5. Time profiles of CuXX ion concentration calculated for various values of T_1.

Results of the experiments carried out with a maximal contrast of the laser pulse are shown in Fig. 3, and in Fig. 6 they are juxtaposed with the calculation for $T_1 = 1$ keV. Note that at times of 1–5 ps the calculated curves have a faster leading edge as compared to the observed one. This is not surprising because the time resolution of the device used is no better than 2 ps and observation of more steep edges is not possible.

Note that the only free parameter in the kinetic model employed is the plasma temperature T_e. The fact that by choosing this parameter one can simultaneously describe two temporal dependences obtained in different spectral ranges indicates both adequacy of the calculation model and possibility of its employment for diagnosing the plasma temperature. We mean the temperature of the main part of electrons because the existence of fast electrons in plasma (with the energies of tens or hundred keV) has no actual effect on the rates of ionisation processes.

In Fig. 6 one can see that our model completely explains the unexpected experimental fact that the pulse of harder SXR from laser plasma has a longer duration then the pulse of softer range. Note once more that this is mainly related to the fact that prior to the gas-dynamic motion the fall in luminescence of one or other ion is determined by the rate of ionisation. This rate falls slower at greater ion charge as long as the electrons from one shell are involved in the process. The rate falls faster when a deeper shell is involved. Since the harder radiation of plasma is caused by just the ions of higher multiplicity, this leads to their longer fluorescence duration as compared to less charged ions.

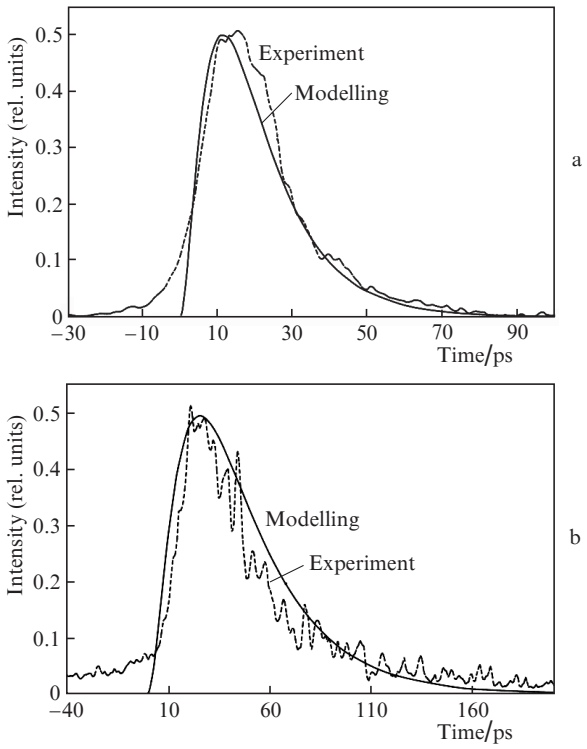

Figure 6. Experimental and calculated data for X-ray radiation in the ranges (a) 0.1–10 keV and (b) 1–10 keV. In both the cases the calculation is performed for $T_1 = 1$ keV.

3.3. Influence of laser pre-pulses of various types on temporal characteristics of the SXR pulses emitted by picosecond laser plasma

Consider the situation where the contrast of laser radiation K_{ASE} is not high. In this case, the pedestal of the laser pulse produces the pre-plasma that radiates in the range 0.1–10 keV. Solution (3) of equation system (1) in this case also gives the possibility to obtain the temporal profile of plasma fluorescence. First, for this purpose system (1) is solved with the initial condition $N_0(0) = N$, $N_1(0) = N_2(0) = 0$ and with the values of W_{ik} calculated for temperature T_0. Then the values $N_i(\tau_{pre})$ are determined from (3) and used as initial conditions for system (1) with the coefficients W_{ik} calculated now for temperature T_1.

The results of calculation for several values of pre-plasma temperature T_0 at fixed temperature T_1 are presented in Fig. 7. By varying T_0 one can study qualitatively the influence of changes in K_{ASE} because the calculation with a higher temperature T_0, obviously, corresponds to a situation with a lower contrast of laser radiation. From Fig. 7 one can see that the pedestal can change (expand) the leading edge of the SXR pulse generated by plasma and should not affect the trailing edge. The influence of pedestal on the leading edge will be clearly seen if the pre-plasma temperature T_0 would be sufficient for ionising the M-envelope of copper ions. In our

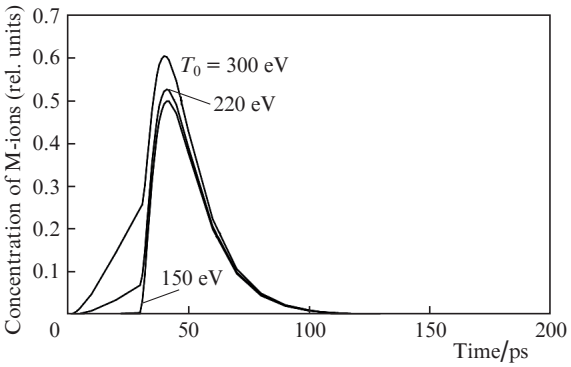

Figure 7. Time profiles of Cu XIX ion concentration calculated for various values of T_0 and fixed temperature $T_1 = 1$ keV at $\tau_{pre} = 30$ ps.

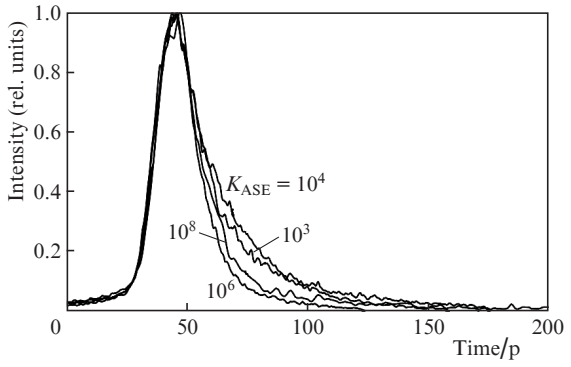

Figure 8. Pulse shape of soft (0.1–10 keV) X-ray radiation emitted by picosecond laser plasma at a maximal contrast $K_{13ns} = 2 \times 10^7$ and various values of K_{ASE}.

experiments no such influence was observed (Fig. 8). This means that the pre-plasma temperature was not above 100–200 eV even at the contrast of 10^3.

However, even not very intensive laser pre-pulse may noticeably affect the SXR pulse generated by plasma if the pre-pulse duration is large, on the order of nanoseconds. Indeed, in this case the pre-plasma produced by the pre-pulse has a chance to expand up to the instant of main pulse arrival and produce a large plasma cloud with the subcritical density $N_e < 10^{21}$ cm^{-3}. Due to the large cloud dimension, a substantial part of energy of the main laser pulse would not reach the region with the critical density and will be absorbed formerly. This will result in that the average density of plasma heated to high temperature will be somewhat less than the critical value. Correspondingly, all ionisation rates will become slower; hence, gradients at the leading and trailing edges of the SXR pulse will be lower. In this case the width of SXR pulse should increase.

For modelling such a situation we employed a picosecond pre-pulse separated from the main pulse by ~13 ns. In experiments, the laser contrast with respect to this pre-pulse was lowered from the ordinary value of 2×10^7 to 10^4 which, as one can see from Fig. 9, indeed resulted in broadening the SXR pulse. In the figure one can also see that the calculation results obtained for $N_e = 5 \times 10^{20}$ cm^{-3} and $T_e = 1000$ eV very well coincide with the experimental results.

Thus, the simple kinetic model suggested is capable of describing the results of performed experiments. It is significant that the employment of this model gives a possibility to

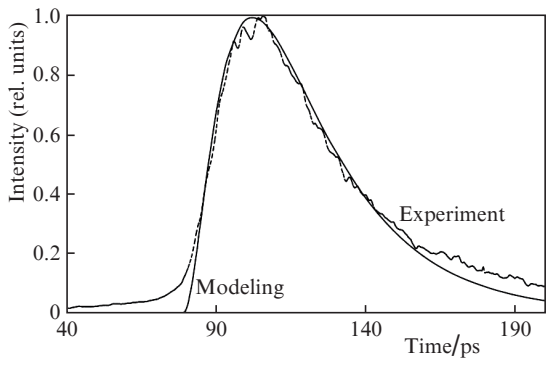

Figure 9. Experimental and calculated data for X-ray radiation in the range 0.1–10 keV. The experiment was carries out at low ($K_{13ns} = 10^3$) and high ($K_{ASE} = 10^8$) contrasts, the calculation corresponds to $T_1 = 1$ keV and $N_e = 5 \times 10^{20}$ cm^{-3}.

predict variations in the generated SXR pulse when one or other parameters of laser pre-pulse chanhes.

4. Conclusions

In the present work, the shape of the short-wavelength pulse generated by picosecond laser plasma was experimentally investigated, and for the first time the method is suggested for controlling its temporal shape by varying the characteristics of the laser pre-pulse or contrast of laser radiation. The simple kinetic model is suggested, capable of describing the results of the experiments performed with picosecond laser pulses. Employment of this model gives a possibility to predict variations in the generated SXR pulse by changing one or other parameters of the laser pre-pulse.

It was experimentally shown that at the laser radiation fluxes of ~10^{18} W cm^{-2}, the deterioration of contrast for the laser pulse pedestal to ~10^3 does not actually affects the shape of the generated SXR pulse, whereas lowering the contrast of the picosecond-duration pre-pulse separated from the main pulse by ~13 ns to the same value makes the SXR pulse longer by 2–3 times.

The unexpected fact has been experimentally established: for targets with $Z \sim 20$–30 under the laser radiation fluxes mentioned above, the pulse of harder laser plasma SXR has a longer duration than the pulse of softer X-ray range. This phenomenon is explained in the frameworks of the kinetic model suggested.

It is interesting that the kinetic model predicts the possibility of controlling the shape of the generated SXR pulse by varying the contrast with respect to the picosecond pedestal or by introducing an additional picosecond pre-pulse. However, this influence will be noticeable in reducing the contrast to 10^2–10^0 where the pre-plasma temperature is sufficient for pre-ionising the M-envelope of target ions. Experiments with such contrasts have not been carried yet.

An important consequence of the employed kinetic model is that for obtaining ultra-short X-ray pulses in plasma heating one should use ultra-contrast laser pulses, with which pre-plasma is not produced. Only in this case the ionisation kinetics will be determined by the solid-state density of electrons, which gives a chance to make the ionisation times shorter by 2–3 orders in magnitude and obtain the duration of the generated X-ray pulse at the level of several or a part of picosecond under optimal conditions (sufficient temperature, prop-

erly chosen spectral range). This conclusion is confirmed by experimental work [26] where, as it follows from our model, just the employment of laser contrast of $\sim 10^{10}$ (second harmonic of laser radiation) provided obtaining the X-ray pulse duration of 0.5–1 ps.

Acknowledgements. The work was partially supported by the Russian Foundation for Basic Researches (Grants Nos 12-02-00489, 13-02-00295, 13-02-00878, 12-02-91169-GFEN_a) and the Program of Fundamental Research No. 2 of the Presidium of RAS.

References

1. McPherson A. et al. *Nature (Ldn)*, **370**, 631 (1994).
2. Donnelly T.D. et al. *Phys. Rev. Lett*., **76**, 2472 (1996).
3. Volkov R.V., Gordienko V.M., Mikheev P.M., et al. *Kvantovaya Elektron*., **34**, 135 (2004) [*Quantum Electron*., **34**, 135 (2004)].
4. Chu H.-H. et al. *Phys. Rev. A*, **71**, 061804(R) (2005).
5. Gordienko V.M., Kurilova M.V., Rakov E.V., et al. *Kvantovaya Elektron*., **37**, 651 (2007) [*Quantum Electron*., **37**, 651 (2007)].
6. Kugland N.L. et al. *Rev. Sci. Insturm*., **79**, 10E917 (2008).
7. Kugland N.L. et al. *Appl. Phys. Lett*., **92**, 241504 (2008).
8. Chen L.M. et al. *Phys. Rev. Lett*., **104**, 215004 (2010).
9. Korobkin Yu.V., Lebo A.I., Lebo I.G. *Kvantovaya Elektron*., **40**, 811 (2010) [*Quantum Electro*n., **40**, 811 (2010)].
10. Zhang L., Chen L.-M., Yuan D.-W., et al. *Opt. Express*, **19**, 25812 (2011).
11. Faenov A.Ya., Magunov A.I., Pikuz S.A., et al. *Pis'ma Zh. Exp. Tekh. Fiz.*, **107**, 351 (2008).
12. Fukuda Y., Faenov A.Ya., Pikuz T., et al. *Appl. Phys. Lett*., **92**, 121110 (2008).
13. Faenov A.Ya., Pikuz T.A., Fukuda Y., et al. *Appl. Phys. Lett*., **95**, 101107 (2009).
14. Fukuda Y., Faenov A.Ya., Tampo M., et al. *Phys. Rev. Lett*., **103**, 165002 (2009).
15. Faenov A.Ya., Pikuz S.A. Jr., Zhidkov A.G., et al. *Pis'ma Zh. Exp. Tekh. Fiz*., **92**, 415 (2010).
16. Kawase K., Kando M., Hayakawa T., et al. *Nucl. Instr. Meth. A*., **637**, S141-S144 (2011).
17. Andreev A.A., Galkin A.L., Kalashnikov M.P., et al. *Kvantovaya Elektron*., **41**, 729 (2011) [*Quantum Electron*., **41**, 729 (2011)].
18. Andreev A.A., Platonov K.Yu. *Kvantovaya Elektron*., **41**, 515 (2011) [*Quantum Electron*., **41**, 515 (2011)].
19. Zigler A., Palchan T., Bruner N., et al. *Phys. Rev. Lett.*, **106**, 134801 (2011).
20. Hayashi Y., Pirozhkov A.S., Kando M., et al. *Opt. Lett*., **36**, 1614 (2011).
21. Gordienko V.M., Dzhidoev M.S., Zhvaniya I.A., et al. *Kvantovaya Elektron*., **42**, 957 (2012) [*Quantum Electron*., **42**, 957 (2012)].
22. Pento A.V., Nikiforov S.M., Simanovskii Ya.O., et al. *Kvantovaya Elektron*., **43**, 55 (2013) [*Quantum Electron*., **43**, 55 (2013)].
23. Murane M.M., Kapteyn H.C., Falcone R.W. *Nucl. Instr. Meth. Phys. Res.*, B**43**, 463 (1989).
24. Niklee P., Kalashnikov M.P., Shnyurer M., et al. *Pis'ma Zh. Exp. Teor. Fiz.*, **62**, 910 (1995).
25. Gallant P., Jiang Z., Chien C.Y., et al. *J. Quantum Spectr. & Radiat. Transf*., **65**, 243 (1999).
26. Gallant P., Forget P., Dorchies F., et al. *Rev. Sci. Instrum*., **71**, 3627 (2000).
27. Maksimchuk A., Nantel M., Ma G., et al. *J. Quantum Spectr. & Radiat. Transf*., **65**, 367 (2000).
28. Bastiani-Ceccotti S., Renaudin P., Dorchies F., et al. *High Energy Density Phys*., **6**, 99 (2010).
29. Brown C.R.D., Hoarty D.J., James S.F., et al. *Phys. Rev. Lett*., **106**, 185003 (2011).
30. Umstadler D. et al. *J. Quantum Spectrosc. Radiat. Transfer*, **54**, 401 (1995).
31. Fournier K.B., Faenov A.Ya., Pikuz T.A., et al. *Phys. Rev. E*, **67**, 016402 (2003).
32. Fournier K.B., Faenov A.Ya., Pikuz T.A., et al. *J. Quantum Spectr. & Radiat. Transf*., **81**, 167 (2003).
33. Fournier K.B., Faenov A.Ya., et al. *J. Phys. B*, **36**, 3787 (2003).
34. Fournier K.B., Faenov A.Ya., Pikuz T.A., et al. *Phys. Rev. E*, **70**, 016406 (2004).
35. Vainshtein L.A., Sobelman I.I., Yukov E.A. *Vozbuzhdenie atomov i ushirenie slektral'nykh linii* (Excitation of Atoms and Spectral Line Broadening) (Moscow: Nauka, 1979).
36. http://spectr-w3.snz.ru.